Desalination and Water Treatment
www.deswater.com

doi: 10.5004/dwt.2022.28572

264 (2022) 244–251
July

Numerical simulation and parameter analysis of Acid Red B migration in river sand

Yiyun An[a,b], Aifang Gao[a,c,*], Zefeng Song[d], Xiaofeng Fang[a], Shaorong Li[a], Boyi Gao[a], Yingying Lian[a], Mingyuan Yu[a], Aiguo Li[a], Bingfei Yang[e]

[a]*School of Water Resources and Environment, Hebei GEO University, Shijiazhuang 050031, China, Tel. +86 311 87208362; emails: llhx2006@126.com (A. Gao), 19832108593@163.com (Y. An), fangxiaofeng@gmail.com (X. Fang), lsrjiayou2021@163.com (S. Li), 2946536680@qq.com (B. Gao), 15175158813@163.com (Y. Lian), marvinyu_1112@163.com (M. Yu), 10067454@qq.com (A. Li)*
[b]*School of Chemistry and Environmental Engineering, China University of Mining & Technology (Beijing), Beijing 100083, China*
[c]*Hebei Center for Ecological and Environmental Geology Research, Hebei Province Collaborative Innovation Center for Sustainable Utilization of Water Resources and Optimization of Industrial Structure, Hebei Province Key Laboratory of Sustained Utilization and Development of Water Resources, Shijiazhuang 050031, China*
[d]*Institute of Resources and Environment, Hebei GEO University, Shijiazhuang 050031, China, Tel. +86 311 87208696; emails: songzefeng@sina.com (Z. Song)*
[e]*Hebei GEO University, Hebei Engineering Research Center for Resource Utilization of Silicate Solid Waste, Shijiazhuang 050031, China, Tel. +86 311 87207272; emails: u7758@126.com (B. Yang)*

Received 7 December 2021; Accepted 10 May 2022

ABSTRACT

In this study, the adsorption and migration characteristics of Acid Red B (AR B) in river sand were investigated using batch and column experiments. The Freundlich equation was used to fit the experimental data of isothermal adsorption. The penetration curves of tracer Cl^- and AR B were simulated by HYDRUS-1D. The results show that with the increase of the initial pH value, the adsorption coefficient K_F in the Freundlich equation decreases gradually, and the adsorption ability of river sand to AR B is weakened. With the increase of initial pH in sand column outflow experimental, the peak value C/C_0 of AR B penetration curve is closer to 1, which indicates that the adsorption is weakened and easy to migrate at higher pH value. The simulation results of non-equilibrium one-site model fitting in HYDRUS-1D show the deterministic coefficient $R^2 > 0.872$ and the root mean square error RMSE < 0.064. The parameters of the model simulation are consistent with the results of the column experimental the breakthrough curves. This model can better describe the migration process of AR B in river sand. It is not conducive to adsorption at higher pH (the smaller K_D), and AR B is easier to migrate with water flow in river sand.

Keywords: Acid Red B; Adsorption; Migration; Breakthrough curve; HYDRUS-1D

1. Introduction

The textile, printing and dyeing industries are closely related to human life. In recent years, with the wide application of various organic dyes, dye-containing wastewater enters the environment in large quantities. However, this kind of wastewater is difficult to degrade naturally, and organic dyes are mostly toxic substances [1–4]. These pollutants entering the soil have become potential hazards in the environment, which can harm the groundwater with the downward migration of soil moisture through leaching and percolation. The pollution of ecological environment

* Corresponding author.

and the threat of human health have increased [5,6]. Organic azo dyes pose a greater risk to the ecological environment, and their migration process between agricultural soil and aquifer media has become a hot issue in environmental scientific research.

Dye wastewater cause serious pollution to the soil environment during production and use. In recent years, the static isothermal adsorption of dye in different soil media has attracted more and more attention [7–11]. Soil solute transport mainly studies the laws and processes of solute transport in the soil environment. A numerical model can simulate the migration process of pollutants after entering the soil, and analyze the influencing factors during the migration process [12,13]. HYDRUS-1D is used to simulate water flow, solute transport and heat transfer in one-dimensional saturated and unsaturated porous media [14]. HYDRUS-1D uses Richards equation, convection-dispersion equation and Galerkin linear finite element method to simulate the water solute transport process under different porous media conditions [13,15,16]. It has been widely used in soil water and nitrogen transport [17–19], soil pollutant transport and groundwater pollution risk assessment [16,20–23]. Yu [24] took oxytetracycline as the target pollutant, obtained parameters through isothermal adsorption test, penetration test, microbial degradation test, and established a solute transport model for vadose zone by using local convective dispersion model, and predicted the penetration of oxytetracycline to vadose zone under various conditions and the possibility of entering groundwater. Zhang et al. [25] used soil column effluent experiments to study the effects of different iron content and ionic strength on the migration of sulfadiazine in iron oxide coated sand, and the results were well simulated by HYDRUS-1D software. However, less simulation model is used to systematically study the migration process, law and mechanism of organic dyes in soil.

In this study, Acid Red B (AR B) is selected as the research object. AR B is a representative azo dye, which is easily soluble in water, and has high COD and chromaticity. It is mainly used for silk textile dyeing, also used in wool, leather, paper, ink, wood and other coloring [26,27]. As the soil is a very complex system under the present experimental conditions, in order to analyze the migration characteristics of AR B under the single factor, the indoor isothermal adsorption experiment and the soil column outflow experiment were carried out with the low reactivity river sand as the medium. The adsorption characteristics of AR B in river sand and its longitudinal migration characteristics in soil profile were analyzed, and the experimental results were numerically simulated by HYDRUS-1D software. The migration behavior of AR B in river sand was discussed, which provided theoretical basis for the prevention and control of organic dyes in soil and groundwater pollution.

2. Material and methods

2.1. Experimental materials and instruments

AR B reagent was purchased from a dye factory in Shijiazhuang, and its structural formula is shown in Fig. 1. The porous medium was natural river sand (from Chifeng City, Inner Mongolia). The density of river sand is 2.59 g/cm^3 and particle size is 0.1–0.25 mm, a curvature coefficient of 1.23 and a non-uniformity coefficient of 1.95. In order to remove some impurities in river sand, the river sand was repeatedly washed with deionized water, which was measured to be close to neutral by pH meter, and then dried at 105°C for later use.

An ultraviolet-visible spectrophotometer (UV-Vis) was used to scan the spectrum of AR B solution in 200–800 nm, and its characteristic wavelength was 515 nm. 10, 20, 30, 40, and 50 mg/L AR B standard solutions were prepared. At the wavelength of 515 nm, the standard curves and equations of absorbance (y) and concentration (x) of AR B are shown in Fig. 2.

2.2. Batch experiment

The adsorption isotherm of AR B was obtained by an isothermal adsorption experiment. The AR B solutions with different concentrations (0.0, 2.0, 5.0, 10.0, 20.0, and 30.0 mg/L) and different pH values (4, 5, and 6) were prepared respectively, and 30 mL AR B solution was mixed with 3 g of river sand, which was added into a 50 mL centrifuge tube (two parallel samples for each experiment). The centrifuge tube was placed on a constant temperature shaker for continuous shaking at 25°C ± 1°C and 150 rpm. Taking off the centrifuge tube after 24 h, placing it in a centrifuge and centrifuging at the speed of 3,000 rpm for 10 min. After centrifugation, supernatant liquid was taken

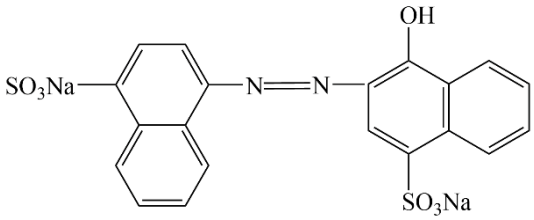

Fig. 1. Molecular structure of Acid Red B.

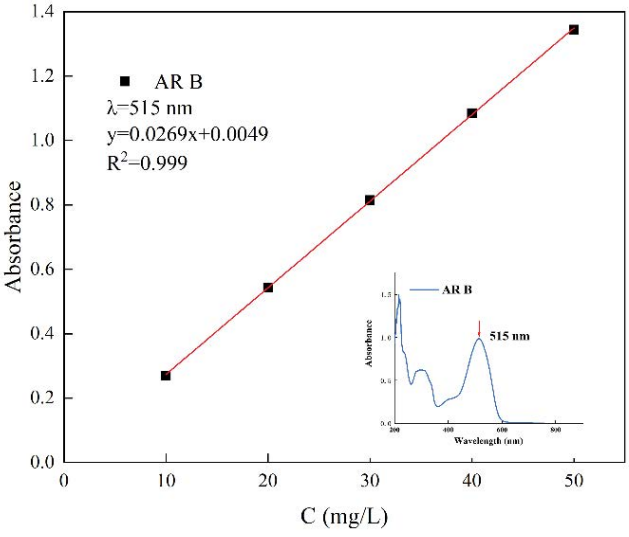

Fig. 2. AR B standard curve.

and the absorbance of AR B was measured by UV-Vis. The dye concentration can be obtained according to the standard curve (Fig. 2). The adsorption capacity of river sand to AR B was obtained by Eq. (1) and the isothermal adsorption curve was drawn.

The adsorption equation of AR B by river sand is:

$$S = \frac{\left(C_0 - C_e\right)V}{m} \tag{1}$$

where S is the adsorption capacity of AR B in river sand (mg/kg) when the adsorption equilibrium is reached; C_0 is the known initial concentration of AR B in solution (mg/L); C_e is the concentration of AR B when adsorption equilibrium is reached (mg/L); V is the volume of solution added to the centrifuge tube (L); m is the mass of added river sand (kg).

2.3. Column experiment

2.3.1. Column experimental device

The experimental device consisted of a liquid storage bottle, peristaltic pump, Plexiglass chromatography column, and UV-Vis (Fig. 3). The inner diameter of the Plexiglass chromatography column was 1 cm and the effective height is 10 cm. The treated river sand was packed into a column by the ultrasonic wet method [28], and the average packing mass of the river sand in the column was determined to be 18.15 g, and the bulk density of the river sand was 2.312 g/cm^3. At the beginning of the experiment, the reserved liquid was pumped into the soil column by a peristaltic pump, and all the experimental flow rates were 1.6 mL/min.

According to Eq. (2), the time for water flowed to pass through one pore volume of the soil column was 31.5 s at a flow rate of 1.6 mL/min.

$$\mathrm{PV} = \frac{vt}{l} \tag{2}$$

where v is pore water velocity (cm/min); t is time (min); l is the length of soil column (cm); PV is a dimensionless time value.

2.3.2. Cl^- tracing experiment

Tracer experiment was carried out with non-reactive chloride ion, and the breakthrough curves (BTCs) of chloride ion in river sand was drawn to determine whether the soil column was filled evenly, and then to determine whether the filling method was feasible. At the same time, the hydraulic parameters of the filled river sand column can be obtained, which provides parameters such as dispersion coefficient for the migration of AR B in river sand. The tracer selected in this experiment was NaCl. After filling the sand column, the deionized water was used to saturate the sand column. When the flow rate of the outlet of the sand column was stable, 20 PV NaCl (0.05 mol/L) solution was put in, then washed with deionized water, and the effluent was collected at the outlet. The concentration of chloride ions was measured by a conductivity meter.

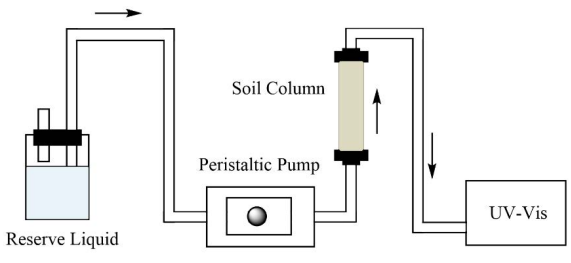

Fig. 3. Schematic diagram of experimental equipment.

2.3.3. Outflow experiment of AR B in river sand

The AR B solutions with different pH (4, 5, and 6) were prepared. Firstly, the sand column was saturated with deionized water, then AR B (20 mg/L) solution was introduced for 20 PV, and then washed with deionized water until the concentration of detected AR B in the effluent was zero. The BTCs under the corresponding conditions was drawn and the influence of river sand on the AR B migration process was analyzed under different pH values.

2.4. Model

2.4.1. Isothermal adsorption model

The Freundlich equation was used to fit the isothermal adsorption curves obtained from static adsorption experiments, and the related parameters K_F and n in the equations were obtained. These parameters can represent the adsorption capacity of river sand to AR B [29,30], and these parameters were used in the migration numerical model. The equation is as follows:

$$S_e = K_F C_e^n \tag{3}$$

where S_e is the adsorption capacity (mg/kg) of soil to AR B in adsorption equilibrium; C_e is the content of AR B in the supernatant at adsorption equilibrium (mg/L); K_F is Freundlich adsorption coefficient, which is related to adsorption capacity. The larger the value, the faster the adsorption rate. n is the adsorption empirical parameter.

2.4.2. Solute transport model

A numerical model of soil water flow and solute transport was established by HYDRUS-1D to simulates the migration process of AR B in the sand column, and to quantitatively describe water flow movement and the reaction of solute in the migration process [31]. It was assumed that the soil was homogeneous and isotropic. In the model, the soil flow model was generalized as a homogeneous isotropic saturated one-dimensional vertical steady flow. Only considering the solute transport process in a one-dimensional uniform medium under adsorption, the convection-dispersion equation (CDE) can be used to describe [14,32], and the equation is as follows:

$$\frac{\partial c}{\partial t} = D\frac{\partial^2 c}{\partial x^2} - v\frac{\partial c}{\partial x} - \rho\frac{\partial s}{\partial t} \tag{4}$$

where c is the solute concentration in liquid phase (mg/L); v is the average pore velocity (cm/min); D is diffusion coefficient (cm²/min); ρ is bulk density (g/cm³); x is the distance (cm); S is the solute concentration adsorbed by unit mass soil (mg/g).

The migration process of Cl^- in river sand was inversed by the HYDRUS-1D model, and the important parameters of solute migration, such as dispersion coefficient D and saturated water content θ_s, were obtained. For non-reactive substances, the adsorption of Cl^- by porous media was almost zero [23], and the solute transport equation can be written as:

$$\frac{\partial c}{\partial t} = D\frac{\partial^2 c}{\partial x^2} - v\frac{\partial c}{\partial x} \tag{5}$$

The migration process of AR B in the river sand column was mainly affected by adsorption, so the one-site model (OSM) was used to describe the solute migration process in river sand. When the soil column is homogeneous soil, the OSM model assumes that the adsorption process is kinetic adsorption and there is no instantaneous adsorption [23,25]. The governing equation is:

$$\frac{\partial \theta c}{\partial t} + \rho\frac{\partial s}{\partial t} = \frac{\partial}{\partial x}\left(\theta D\frac{\partial c}{\partial x}\right) - \frac{\partial qc}{\partial x} \tag{6}$$

$$\rho\frac{\partial s}{\partial t} = \alpha\rho\left[S_e - S\right] \tag{7}$$

$$S_e = K_d c \tag{8}$$

where q is water flux (cm/min); S_e is the solute concentration adsorbed per unit mass of soil at adsorption equilibrium (mg/g); S is solute concentration of kinetic adsorption (mg/g); α is the first-order rate constant (min) describing the kinetic adsorption process.

3. Results and discussion

3.1. Sorption isotherms

3.1.1. Effects of pH on adsorption of AR B in river sand

The nonlinearity of the adsorption isotherm indicates that the adsorption capacity of river sand to AR B is related to the concentration of solute. When the concentration of AR B solution is low, the high energy adsorption points on the surface of river sand first binds to AR B, and the adsorption energy is strong. When the concentration of AR B increases, the adsorption capacity increases. However, because of the limited adsorption point, the adsorption becomes saturated and the adsorption capacity eventually tends to a constant value.

Table 2 shows the adsorption capacity of river sand to AR B for 24 h under different pH values and initial AR B concentrations at 25°C. From Table 2, with a pH of 4~6, pH is higher, river sand to AR B adsorption capacity is lower. When the AR B concentration is 30 mg/L, the adsorption capacity of river sand is 49.22 mg/kg (pH 4), 36.21 mg/kg (pH 5), 7.96 mg/kg (pH 6). The pH value of the solution affects the surface charge state of the river sand, as a result, the adsorption behavior of AR B in river sand is affected. The adsorption capacity of river sand to AR B varies greatly under different pH, that is, when pH = 4, the adsorption capacity is the largest, and when pH = 6, the adsorption capacity is the smallest. This reason is the lower the pH value, the more positive charge on the surface of the adsorbent is gathered, which produces a larger potential difference with the AR B ionized in aqueous solution and increases the electrostatic attraction [33], so it is easier to be adsorbed on the adsorbent surface.

3.1.2. Data fitting of AR B adsorption in river sand

The Freundlich equation was used to fit the adsorption data in Table 3, and the relevant adsorption parameters were obtained. The fitting results are shown in Table 3 and Fig. 4. The isothermal adsorption equation Freundlich can well fit the adsorption characteristics of river sand to AR

Table 2
Adsorption capacity of river sand to AR B under different pH and initial concentration (mg/kg)

pH	Initial AR B concentration (mg/L)				
	2	5	10	20	30
6	0.260	1.450	2.193	4.981	7.955
5	5.093	11.487	17.063	25.799	36.208
4	7.695	14.275	22.268	38.253	49.219

Table 1
Laboratory instrument

Instrument	Type	Manufacturer
UV-Vis	2802	UNICO
Reciprocal shaker	SHZ BS	Shanghai Bingyue Electronic Co., Ltd., China
Peristaltic pump	BT100-2J	Baoding LanGe Constant Flow Pump Co., Ltd., China
Centrifuge	LDZ5-2	Beijing Medical Centrifuge Factory, China
pH meter	PHSJ-4A	Shanghai INESA Scientific Instrument Co., Ltd., China
Ultrasonic cleaner	KQ-500DE	Kunshan Ultrasonic Instruments Co., Ltd., China
Ultrapure water machine	FST-WL-10	Shanghai Fushite Instrument Equipment Co., Ltd., China
Column	Plexiglass 100 mm × 10 mm	Shanghai Tongxing Glass Instrument Co., Ltd., China

B. The parameter values K_F, n, and R^2 obtained by model fitting are given in Table 3. The adsorption isotherm of river sand to AR B was successfully described by the equation, and the R^2 value fitted by the Freundlich equation was greater than 0.991. K_F can be used to evaluate the adsorption affinity of river sand on AR B. The K_F values differ greatly in the fitting results under different pH values, indicating that the adsorption capacity of river sand to AR B varies greatly. At pH = 4, the binding affinity is the highest (K_F = 6.259 L/kg), while at pH = 6, the binding affinity is the lowest, decreasing to be 0.188 L/kg. In a word, with the increase of pH, the adsorption of river sand to AR B decreases. The adsorption capacity of river sand to AR B is negatively correlated with pH value. As can be seen from Fig. 1, AR B is a polar molecule that ionizes to produce negatively charged sulfonic acid groups in aqueous solution. The zero potential (pH_{pzc}) of river sand is about 7.19. When pH < 7.19, the surface of the medium is positively charged [34]. The positively charged river sand on the surface can produce electrostatic attraction with the negatively charged sulfonic acid group [35]. The higher the acidity is, the higher the positive charge on the surface of river sand is. The electrostatic attraction between river sand and AR B is the largest, and the adsorption amount of AR B is also the largest. In relatively high pH solutions, the river sand surface is prone to hydroxylation, and AR B is an anionic dye, which weakens the adsorption capacity of the river sand to AR B.

Table 3
Fitting parameters of the adsorption isotherm model (Freundlich)

pH	K_F	n	R^2
6	0.188	1.108	0.993
5	4.384	0.639	0.991
4	6.259	0.642	0.997

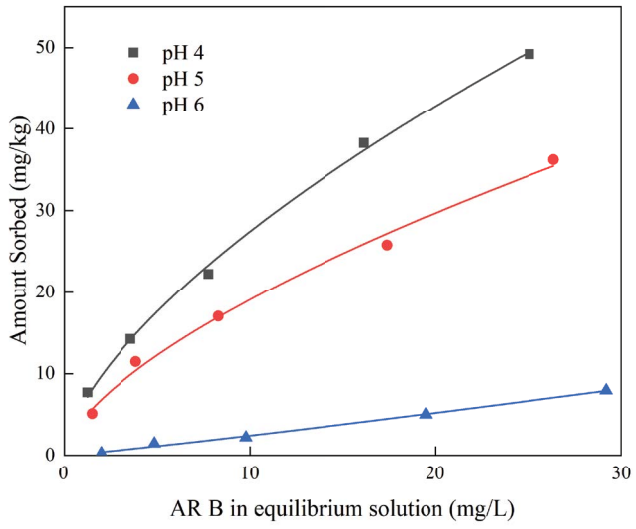

Fig. 4. Sorption isotherms for river sand to AR B at different pH values.

3.2. Breakthrough curves

3.2.1. Tracer breakthrough curves and model inversion parameters

In an indoor soil column simulation device, the NaCl solution was leached at a certain flow rate with the low reactive substance Cl^- as the tracer, and the Cl^- concentration in the effluent was measured at the upper end of the glass column device, thus obtaining the BTCs of Cl^- in the river sand column (Fig. 5). The migration of chemical substances in porous media is a complex process, and the non-reactive substance Cl^- is not affected by chemical disequilibrium during the migration process. Therefore, the symmetrical or tailing phenomenon of the penetration curve can be used to determine whether physical disequilibrium exists in the migration process [36]. It can be seen from Fig. 5 that the BTCs of Cl^- in river sand is symmetrical and there is no tailing. The river sand in the column is uniformly filled, and there are no macropores and preferential flows. It shows that there is no physical disequilibrium phenomenon under this experimental condition, and the influence of immobile water on the migration of Cl^- and AR B in porous media can be ignored [23]. Therefore, OSM can be used to describe the migration behavior of organic dye AR B in river sand.

The tracer curve of Cl^- is fitted by HYDRUS-1D software. Soil hydraulic characteristic parameters and solute characteristic parameters are needed in establishing the model. The medium used in this experiment is river sand, so the soil hydraulic characteristic parameters directly use the relevant parameters of a sand medium in UNSODA database in the HYDRUS-1D software (Table 4).

The BTCs of tracer Cl^- in river sand are fitted by the CDE model. Because there is almost no adsorption of Cl^- in the process of river sand migration, the adsorption distribution coefficient given in the model K_D = 0 [32,37], in which the initial value of flow velocity is set to 2.038 cm/min. Saturated water content θ_s and dispersion coefficient D are obtained by simulation inversion (Table 4), and the fitting curve is shown in Fig. 5. The correlation coefficient R^2 of the model fitting results is 0.999, and the root mean square error RMSE

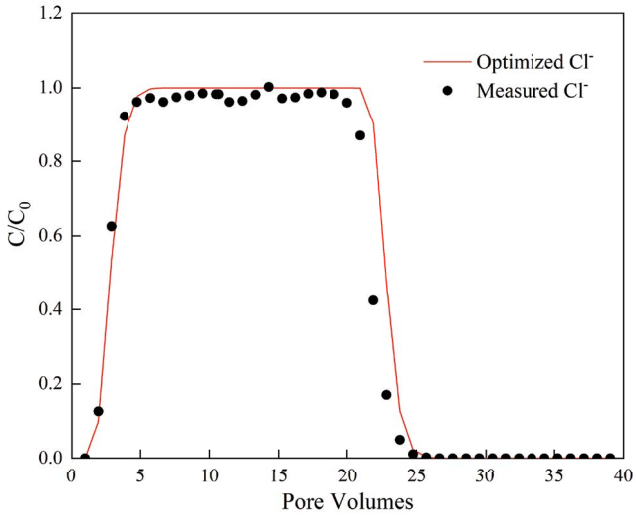

Fig. 5. Breakthrough curves and fitting curve of Cl^-.

is 0.008. It shows that the migration of Cl^- in river sand is well fitted by the CDE model. The parameters obtained from the fitting will be used to simulate the migration of AR B in river sand. Xu et al. [22] fitted the penetration curve of Br^- in the unbroken soil column and applied the D and θ_s parameters to the numerical simulation of Ciprofloxacin Star transport using the CDE model. Our research and the result of Xu et al. [22] are comparable and reasonable.

3.2.2. AR B breakthrough curves and model parameter determination

The breakthrough experiment of AR B at different initial pH values and the effect of pH on adsorption of river sand to AR B are shown in Fig. 6. It can be seen from Fig. 6 that the concentration of AR B at the outlet is zero at the initial stage of adsorption. With the continuous penetration of the solution, the adsorption continues and the concentration of the effluent increases gradually. When it increases to a certain extent, the BTCs tends to be gentle. Under the continuous elution of deionized water, the concentration of effluent begins to decrease and gradually approaches zero. From Fig. 6, when the input concentration of AR B is 25.85 mg/L, the adsorption rate of river sand to AR B becomes lower and lower as the initial pH of the solution increases from 4 to 6. This phenomenon is consistent with the conclusion is obtained by the Freundlich model in the isothermal adsorption experiment, that is, the parameter K_F decreases with the increase of pH value. In the later stage of the experiment, the sand column was continuously washed with deionized water, and AR B adsorbed by river sand entered the desorption stage. When the pH value was 6, the effluent concentration first tended to zero, and the retention effect was the worst [22]. With the increase of pH, the adsorption of AR B by river sand is weakened, which indicates that at higher pH, AR B is easier to migrate, the penetration ability is better, and it is easier to be desorbed in river sand.

Table 4
Fitting parameters of Cl^- breakthrough curves

Column	River sand
Model	CDE
θ_s (cm^3/cm^3)	0.491
ν (cm/min)	2.038
D (cm^2/min)	0.257
R^2	0.999
RMSE	0.008

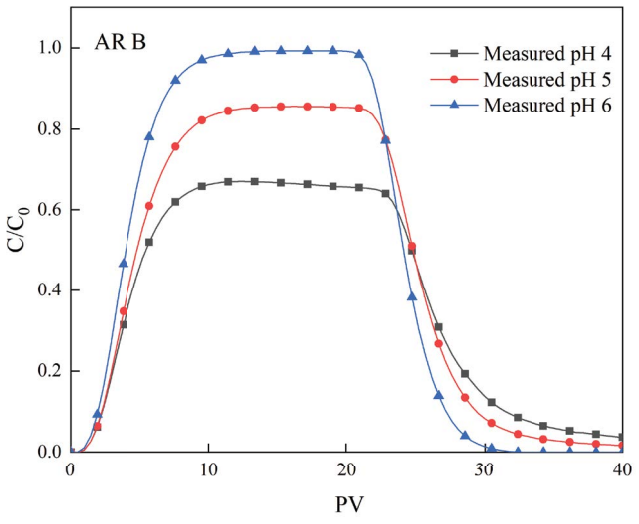

Fig. 6. Breakthrough curve of AR B for different pH.

Solution pH will cause changes in surface charge of river sand and dissociation of AR B, affect the adsorption behavior of AR B by river sand, and then affect the migration process of AR B. Under the lower pH condition, more positive charge is accumulated on river sand surface, while AR B has a negatively charged sulfonic acid group, so the electrostatic attraction is greater. When the solution pH is higher, the electrostatic attraction between river sand and AR B decreases, and AR B migrates more easily with water flow. Our result is consistent with that of Li [38]. The adsorption capacity of river sand to sulfaethoxazole (SMX) decreases with the increase of pH value, mainly because hydroxyl groups on the surface of river sand have negative charges in the protonation process, which is conducive to the electrostatic adsorption of SMX [38].

The saturated moisture content θ_s and dispersion coefficient D were obtained by fitting the BTCs of tracer Cl^- using the CDE model (Table 4). OSM coupled with Freundlich nonlinear adsorption was used to fit the BTCs of AR B in river sand column under different pH values. Parameters required by the simulation mainly include adsorption parameters K_D and n and first-order rate constant α, and the solutions of these three parameters are not unique. Therefore, K_F and n (Table 3) obtained from the Freundlich model in the isothermal adsorption experiment are taken as reference values, and different initial values of the three parameters are substituted into the model. The simulation results of the model are analyzed until the error between the simulation results and the measured values is very small. The BTCs of AR B in river sand column under different pH simulated by HYDRUS-1D is shown in Fig. 7, and the parameters obtained by model inversion are listed in Table 5.

It can be seen from Table 5 that the deterministic coefficients R^2 obtained by fitting are all greater than 0.870, especially under the conditions of pH 6 and 5, and their deterministic coefficients are greater than 0.96, indicating that the HYDRUS-1D model can well simulate the migration of AR B in river sand column. RMSE is used to characterize whether the model fits well. It can be found that

Table 5
Fitting parameters of AR B breakthrough curves for different pH in river sand

pH	AR B (mg/kg)	K_D	n	α	R^2	RMSE
6	25	0.100	0.883	0.986	0.994	0.013
5	25	1.317	0.446	0.237	0.964	0.032
4	25	2.689	0.880	0.032	0.872	0.064

RMSE is less than 0.07 and close to 0, indicating that the deviation between the simulated value and the measured value is small, and the model prediction is successful. OSM can well describe the migration behavior of AR B in river sand. Adsorption partition coefficient K_D can represent the adsorption strength of AR B in river sand to some extent. The parameters obtained from the model inversion (Table 5) show that the K_D value increases with the decrease of the pH value. This indicates that the adsorption capacity is enhanced [16]. Zhang [39] also used OSM model to simulate the migration process of Sulfadiazine in quartz sand under different pH conditions. The lower the pH is, the larger the simulated K_D is. The K_D value is the maximum when the pH is 4, indicating that quartz sand surface has the largest adsorption effect on Sulfadiazine. In our study, when the pH value is equal to 6, K_D value is only 0.1, and it can be seen from Fig. 6 that with the increase of pH value, the peak value of effluent concentration C/C_0 is getting closer and closer to 1, which is 0.67 (pH = 4), 0.86 (pH = 5), and 0.99 (pH = 6), respectively. When pH value is 6, the peak value of effluent concentration reaches 0.99, which is close to the initial influent concentration of solute. This indicates that the adsorption capacity of river sand to AR B (pH = 6) is smaller than that of pH values of 4 and 5, and the sand column quickly reaches the adsorption saturation state. The adsorption distribution coefficient K_D obtained by the HYDRUS-1D model is smaller than that measured by the isothermal adsorption experiment, which indicates that the adsorption capacity of river sand is weak during the migration of river sand. This may be due to the short contact time between the AR B and the river sand in the migration experiment and the dye solution has been flowing all the time, which leads to insufficient contact and reduced adsorption strength [22]. However, the contact time between river sand and AR B is longer (24 h) in the isothermal adsorption experiment, so the adsorption capacity is larger.

There are several factors that affect the adsorption of AR B by river sand, such as particle size, pH value, ion strength, water flow rate, cation exchange capacity, and so on. This study only considers the influence of pH on the adsorption and migration of AR B in river sand. Therefore, it is necessary to further analyze the influence of other factors on AR B migration in future studies. The adsorption and migration characteristics of AR B in river sand still need to be supplemented in these aspects.

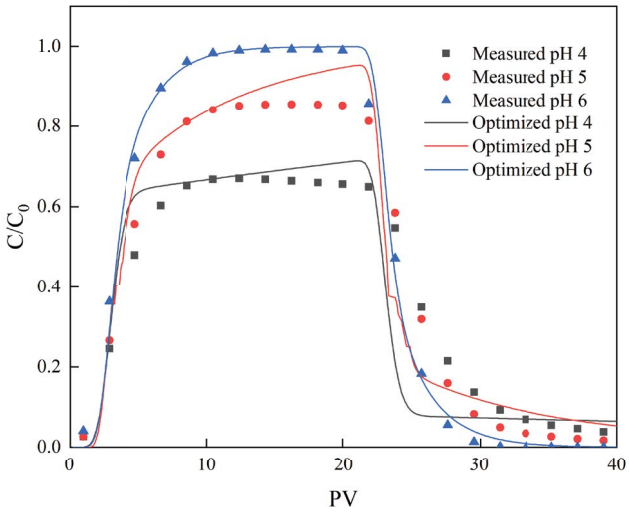

Fig. 7. Breakthrough curve and fitting curve of AR B for different pH.

4. Conclusions

- The experimental data isothermal adsorption is fitted by a nonlinear adsorption model. When the isothermal adsorption curve is fitted by the Freundlich equation, the R^2 is greater than 0.99, and the fitting effect of the Freundlich equation is good. The parameter K_F in the Freundlich equation decreases with the increase of pH, which indicates that the larger the pH, the more unfavorable the adsorption is.
- The BTCs of soil column outflow experiment was simulated by the HYDRUS-1D model, and the saturated moisture content θ_s = 0.491 and dispersion coefficient D = 0.257 of hydraulic parameters were obtained by fitting the Cl^- tracer curve of the CDE model in the software. Using the OSM model, the adsorption migration of AR B in river sand column with different pH values (4, 5, and 6) was analyzed. The R^2 values of the three groups of experimental fitting curves were 0.994, 0964, 0.872, and the RMSE values were 0.013, 0.032, and 0.064. The fitting results show that the mathematical model is consistent with the actual situation.
- The migration characteristics of AR B in river sand are obvious at different pH values. With the increase of pH value, the peak value of outflow C/C_0 is closer to 1. With the changing of pH, the parameter K_D obtained by model inversion is consistent with the change trend of parameter K_F obtained by fitting Freundlich in the isothermal adsorption experiment. The results show that it is not conducive to the adsorption of AR B by river sand at higher pH, which is easier to be desorbed and the migration ability is enhanced.

Declaration of competing interest

The authors declare that they have no known competing financial interests or personal relationships that could have appeared to influence the work reported in this paper.

CRediT author statement

Yiyun An: Experimental implementation, Data curation, Formal analysis, Validation, Writing – original draft. Aifang Gao: Conceptualization, Methodology, Formal analysis, Writing – Reviewing and Editing, Supervision, Project administration. Zefeng Song: Writing-Reviewing and Editing, Supervision. Xiaofeng Fang: Data curation, Writing-Reviewing and Editing. Shaorong Li: Experiment, Writing-Editing. Boyi Gao: Writing-Reviewing and Editing. Yingying Lian: Experimental implementation, Data curation. Mingyuan Yu: Experimental implementation, Data curation, Validation. Aiguo Li: Writing – Reviewing and Editing. Bingfei Yang: Writing – Reviewing and Editing.

Acknowledgments

The work is supported by Project on Provincial Innovative Entrepreneurship Training for College Students (S202010077009), Local science and technology development fund projects guided by the central government (V1624263512908), Science and Technology Project of Hebei Education Department (ZD2020135), and Overseas Talents Introduction Funded Project of Hebei Province (C20200308).

References

[1] G. McMullan, C. Meehan, A. Conneely, N. Kirby, T. Robinson, P. Nigam, I.M. Banat, R. Marchant, W.F. Smyth, Microbial decolourisation and degradation of textile dyes, Appl. Microbiol. Biotechnol., 56 (2001) 81–87.
[2] Y. Cheng, Q. Zhou, Q. Ma, Y. Wang, Progress in treating methods of wastewater containing dyes, Tech. Equip. Environ. Pollut. Control, 4 (2003) 56–60.
[3] U. Pagga, D. Brown, The degradation of dyestuffs: part II behavior of dyestuffs in aerobic biodegradation tests, Chemosphere, 15 (1986) 479–491.
[4] Q. Zhou, C.E. Gibson, Y.M. Zhu, Evaluation of phosphorus bioavailability in sediments of three contrasting lakes in China and the UK, Chemosphere, 42 (2001) 221–225.
[5] Y. Wang, Z. Zhao, Y. Wang, J. Hua, D. Zhang, H. Zhang, S. Jiao, Study on the pollution characteristics of typical textile dyeing sludge (TDS) in China, J. Ecol. Rural Environ., 36 (2020) 96–102.
[6] J. Zhang, J. Wei, Y. Lü, L. Duan, L. Liu, J. Wang, S. Meng, Occurrence and ecological risk assessment of typical persistent organic pollutants in Hengshui Lake, Environ. Sci., 41 (2020) 347–357.
[7] Q. Zhou, Transporting models of reactive X-3B red dye in water-soil-crop continuums, Chin. J. Ecol., 13 (2002) 129–132.
[8] B. Qu, J. Zhou, X. Xiang, C. Zheng, H. Zhao, X. Zhou, Adsorption behavior of azo dye CI Acid Red 14 in aqueous solution on surface soils, J. Environ. Sci., 20 (2008) 704–709.
[9] S. Jagdish, K. Gagndeep, Freundlich, Langmuir adsorption isotherms and kinetics for the removal of malachite green from aqueous solutions using agricultural waste rice straw, Int. J. Environ. Stud., 4 (2013) 250–258.
[10] B. Qu, Adsorption, Contamination Diagnosis and Associated Bioremediation of C.I. Acid Red 14 in Soil, Dalian University of Technology, Dalian, 2008.
[11] X. Shi, C. Tang, Y. Zhang, Y. Wu, Y. Zhang, Comparative study on adsorption of organic cation dye wastewater by typical soil minerals, J. Green Sci. Technol., 2 (2020) 65–70.
[12] J.M. Kohne, S. Kohne, J. Simunek, Multi-process herbicide transport in structured soil columns: experiments and model analysis, J. Contam. Hydrol., 85 (2006) 1–32.
[13] W. Li, J. He, L. Liu, P. Gao, Y. Ji, Application of HYDRUS-1D software in groundwater contamination risk assessment, Chin. Environ. Sci., 33 (2013) 639–647.
[14] J. Simunek, J. Simunek, M.T.V. Genuchten, M. Sejna, J. Simunek, M. Genuchten, M. Šejna, The HYDRUS 1D Software Package for Simulating the One-dimensional Movement of Water, Heat, and Multiple Solutes in Variably Saturated Porous Media, Hydrus Software 68, 2005.
[15] J. Li, R. Zhao, Y. Li, L. Chen, Modeling the effects of parameter optimization on three bioretention tanks using the HYDRUS-1D model, J. Environ. Manage., 217 (2018) 38–46.
[16] B. Zhang, Q. Lin, S. Xu, Effects of Cd/Cu/Pb on adsorption and migration of sulfadiazine in soil, Acta Petrol. Sin., 55 (2018) 1120–1130.
[17] Q. Cao, Y. Gong, Simulation and analysis of water balance and nitrogen leaching using HYDRUS-1D under winter wheat crop, Plant Nutr. Fertilizer Sci., 9 (2003) 139–145.
[18] J. Bi, J. Zhang, X. Chen, A. Zhu, J. Feng, Simulation of soil water leaching and nitrate-n loss with leachate in the field using HYDRUS-1D model, Rural Eco-Environ., 20 (2004) 28–32.
[19] T.B. Ramos, J. Simunek, M.C. Goncalves, J.C. Martins, A. Prazeres, N.L. Castanheira, L.S. Pereira, Field evaluation of a multicomponent solute transport model in soils irrigated with saline waters, J. Hydrol., 407 (2011) 129–144.
[20] A. Elmi, J.S. Abou Nohra, C.A. Madramootoo, W. Hendershot, Estimating phosphorus leachability in reconstructed soil columns using HYDRUS-1D model, Environ. Earth Sci., 65 (2012) 1751–1758.
[21] S. Zhang, M. Jin, Q. Sun, Experiment and numerical simulation on transportation of ammonia nitrogen in saturated soil column with steady flow, Procedia Environ. Sci., 10 (2011) 1327–1332.
[22] X. Xu, Q. Lin, S. Xu, Adsorption transport and parameter analysis of ciprofloxacin in quartz sand, Acta Sci. Circum., 6 (2016) 2085–2094.
[23] B. Zhang, Q. Lin, S. Xu, Characteristics and simulation of transport of sulfadiazine in undisturbed soil columns, Acta Pedol. Sin., 55 (2018) 879–888.
[24] C. Yu, Migration and Transformation of Oxytetracycline in Aeration Zone and Numerical Simulation, Chang An University, Xi'an, 2017.
[25] H. Zhang, Q. Lin, S. Xu, Characteristics of sulfadiazine migration in iron oxide coated sand and a comparison with simulation results, Chin. Environ. Sci., 39 (2019) 4712–4721.
[26] D. Cao, M. Yu, R. Liu, G. Han, Q. Zhang, Y. Xu, J. Hu, W. Zhang, S. Zhang, Identification of Acid Red B decolorization bacteria and the theoretical back ground of the decolorization kinetics, J. Saf. Environ., 17 (2017) 2371–2375.
[27] Y. Yang, X. Hu, Isolation and identification of a salt-tolerant bacteria Strain BY-2 for Acid Red B degradation, J. Chem. Eng. Chin. U., 30 (2016) 734–740.
[28] Z. Song, Y. Wang, Y. Yang, X. Song, Y. Li, Migration of colloids and their adsorption of typical steroid estrogens, Chin. J. Environ. Eng., 13 (2019) 1082–1091.
[29] T. Madrakian, A. Afkhami, H. Mahmood-Kashani, M. Ahmadi, Adsorption of some cationic and anionic dyes on magnetite nanoparticles-modified activated carbon from aqueous solutions: equilibrium and kinetics study, J. Iran. Chem. Soc., 10 (2013) 481–489.
[30] C. Weng, Y. Pan, Adsorption of a cationic dye (methylene blue) onto spent activated clay, J. Hazard. Mater., 144 (2007) 355–362.
[31] M. Th. Van Genuchten, Non-Equilibrium Transport Parameters from Miscible Displacement Experiments, United States Department of Agriculture, 1981.
[32] J. Zhan, W. Li, Z. Li, G. Zhao, Indoor experiment and numerical simulation study of ammonia-nitrogen migration rules in soil column, J. Groundwater Sci. Eng., 6 (2018) 205–219.
[33] Y. Wang, L. Yuan, H. Kang, Functional quaternary ammonium salt modified montmorillonite and its adsorption performance of Congo red dyes in water, Environ. Prot. Chem. Ind., 42 (2022) 87–93.
[34] H. Chen, H. Shan, S. Peng, J. Huang, D. Liao, Z. Yan, Hydrochemical influences on arsenic adsorption by river sand, Acta Sci. Circumst., 41 (2021) 2727–2739.
[35] R.C. Xu, Haiyan, S. Ping, Binding and adsorption of dye acid red-B by lignite from the mining sewage, J. Saf. Environ., 11 (2011) 35–38.
[36] X. Ji, J. Sun, Modeling copper transport in saturated sandy loam column, Environ. Sci. Technol., 35 (2012) 14–17.
[37] Z. Shao, Q. Lin, S. Xu, Effect of silica colloids on adsorption and migration of sulfadiazine in soil relative to ionic intensity, Acta Pedol. Sin., 55 (2018) 411–421.
[38] G. Li, Simultaneous Adsorption Performance of Sulfamethoxazole, Cr(VI) and Dimethyl Phthalate Different Substrates, South China Agricultural University, Guangzhou, 2018.
[39] H. Zhang, Characteristics of Sulfadiazine and Cadmium Migration in Iron Oxide Coated Sand and a Comparison with Simulation Results, Qingdao University, Qingdao, 2020.